



Originally published as:

Zemke, K., Liebscher, A., Wandrey, M. (2010): Petrophysical analysis to investigate the effects of carbon dioxide storage in a subsurface saline aquifer at Ketzin, Germany (CO2SINK). - International Journal of Greenhouse Gas Control, 4, 6, 990-999

DOI: [10.1016/j.ijggc.2010.04.008](https://doi.org/10.1016/j.ijggc.2010.04.008)

Petrophysical analysis to investigate the effects of carbon dioxide storage in a subsurface saline aquifer at Ketzin, Germany (CO<sub>2</sub>SINK)

Kornelia Zemke\*, Axel Liebscher, Maren Wandrey and the CO<sub>2</sub>SINKGroup

Helmholtz Centre Potsdam, GFZ German Research Centre for Geosciences, Centre for CO<sub>2</sub> Storage, Telegrafenberg, 14473 Potsdam, Germany

\*Corresponding author: zemke@gfz-potsdam.de

### ***Abstract***

To test the injection behaviour of CO<sub>2</sub> into brine-saturated rock and to evaluate the dependence of geophysical properties on CO<sub>2</sub> injection, flow and exposure experiments with brine and CO<sub>2</sub> were performed on sandstone samples of the Stuttgart Formation representing potential reservoir rocks for CO<sub>2</sub> storage. The sandstone samples studied are generally fine-grained with porosities between 17 and 32 % and permeabilities between 1 and 100 mD.

Additional batch experiments were performed to predict the long-term behaviour of geological CO<sub>2</sub> storage. Reservoir rock samples were exposed over a period of several months to CO<sub>2</sub>-saturated reservoir fluid in high pressure vessels under in situ temperature and pressure conditions. Petrophysical parameters, porosity and the pore radius distribution were investigated before and after the experiments by NMR (Nuclear Magnetic Resonance) relaxation and mercury injection. Most of the NMR measurements of the tested samples showed a slight increase of porosity and a higher proportion of large pores.

### ***Keywords***

CO<sub>2</sub> storage, CO<sub>2</sub>-water-rock interaction, flow experiments, petrophysical analysis, pore size distribution

## ***1 Introduction***

Saline aquifers are the most promising option for geological storage of CO<sub>2</sub> to avoid its emissions into the atmosphere and to mitigate climate change. However, injection of CO<sub>2</sub> into the brine-filled reservoir rocks, mostly sandstones, leads to chemical and physical reactions in the reservoir, which are controlled by fluid and rock composition, pressure and temperature conditions in the reservoir and also injection conditions (Rochelles, 2004). The effect of CO<sub>2</sub> injection on physical rock properties in general is not well established. Fluid-rock interactions can lead to the dissolution of minerals in CO<sub>2</sub>-bearing pore fluids, the precipitation of minerals with related reduction or plugging of the pore space, and the drying and disintegration of clay minerals (e.g., Förster et al., 2006). These processes may result in changes of porosity geometry and distribution, effective permeability, and capillary entry conditions, which all influence and change the petrophysical and fluid transport properties. Laboratory batch and flow-through experiments (e.g., Pearce et al., 2000) as well as field scale in situ CO<sub>2</sub> experiments (e.g., Hovorka, 2004; Worden and Smith, 2004) have been performed to study petrophysical effects of CO<sub>2</sub>-water-rock interactions. However, the duration of these experiments was generally too short to address the long-term effects of water-rock interactions.

To determine the effects of injected CO<sub>2</sub> on the petrophysical properties of brine-filled reservoir rocks, sandstone samples of the Upper Triassic Stuttgart Formation, Germany, were studied experimentally under simulated in situ conditions using flow-through and batch methods. The Stuttgart Formation is one of the potential reservoir formations in Germany and is the target horizon of the first European on-shore storage project at Ketzin (Brandenburg, Germany). Here, food grade carbon dioxide ( $\geq 99.9\%$  purity) is injected into sandstone layers of the Stuttgart Formation since June 2008 (Würdemann et al., 2009). The reservoir sandstones at Ketzin are at about 630 to 650 m depth with initial reservoir conditions of  $\sim 33^\circ\text{C}$  and 6.2 MPa. One primary objective of the laboratory program associated with the Ketzin storage activities is the assessment of the effects of long-term CO<sub>2</sub> exposure on reservoir rocks in order to predict the long-term behaviour of geologically stored CO<sub>2</sub>. The here presented experiments extend the work of Schütt et al. (2004) on petrophysical parameters, the first flow experiments with CO<sub>2</sub> and brine on cores from the abandoned wells of the former gas storage operations in Ketzin (Förster et al.; 2006), and the flow experiments on reservoir rocks from the newly drilled well Ktzi 202 (Kummerow; personal communication). The experimental studies intend to provide basic input parameters for the interpretation of the well logging and geophysical monitoring program at Ketzin.

Therefore, reservoir rock samples were exposed to CO<sub>2</sub> and brine in high-pressure vessels under in situ temperature and pressure conditions over different time scales. The composition of the brine is representative of the formation fluid of Ketzin and is described in Förster et al. (2006). Here we present the results from petrophysical measurements. Results on microbiological and geochemical processes will be presented in a companion paper.

## 2 *Methodology*

### 2.1 Sample description and preparation

The studied sandstone samples of the Triassic Stuttgart Formation of Germany come from outcrops in Thuringia, Hessen, and Baden Württemberg as well as from well Ktzi 202 of the Ketzin test site in Brandenburg (Table 1). They represent a range in mineralogical and petrological parameters and thus may be taken as representative for the German Stuttgart Formation.

For density measurements with Helium, porosity determination, NMR measurements and mercury injection sample pieces of the outcrop material were taken (Table 1). For flow measurements, cores ( $\varnothing$  50 mm x 100 mm) were prepared out of the outcrop samples by drilling with air, because some samples disintegrated during contact with water. One of these drilled cores (S13) was then used for the presented flow experiment with brine and CO<sub>2</sub>.

For the first run of CO<sub>2</sub> exposure experiments three sandstone cores ( $\varnothing$  50 mm x 100 mm) were prepared from a quarry in Baden Württemberg (BW3 in Table 1) with 20% porosity and 30 to 100 mD brine permeability. The samples are fine grained, well sorted sandstone. The cement is mostly shaly-ferritic, but occasionally siliceous or dolomitic. These experiments include brine flow and pressure loading measurements before and after CO<sub>2</sub> exposure.

The second run of exposure experiments were conducted with 7 freshly acquired samples from well Ktzi 202, drilled in 2007 (Table 1, Fig. 3). Since these exposure experiments are also studied microbiologically and geochemically, any contamination of the samples and vessels had to be minimised or excluded. The outer core sections were contaminated with drilling mud, as shown by tracer fluorescence (Wandrey et al., 2010, this issue), inner core sections were used for the exposure experiments in order to avoid the contamination with microorganisms, as well as organic and inorganic mud components. Planned experiments with the mechanical testing system (MTS) required plan parallel cylindrical cores ( $\varnothing$  50 mm x 100 mm) which were prepared by drilling long-axis parallel in an Argon stream to minimise oxidation influences by using sterilised equipment.

### 2.2 Experimental methods

#### Flow experiments – mechanical testing system MTS

For the fluid flow experiments a temperature-controlled pressure vessel was used (Fig. 1). In this vessel, the confining pressure (simulating lithostatic pressure) acted on a Perfluoroalkoxy PFA-jacket around the sample (maximal 140 MPa). The mechanical testing system (MTS) has a triaxial cell that allows variable axial loading (maximal 4600 kN) and thus the determination of axial and lateral strain (Schütt et al., 2004). The fluid pressure, which simulates the hydrostatic pressure plus the injection pressure, was applied through the sliced end caps, and was generated separately. The end caps contain Piezo ultrasonic transducers for compression and shear waves (500 kHz) and thus allow measuring P- and S-waves velocities. The end caps also simultaneously act as current electrodes for four-electrode electrical resistivity measurements. The system setup is designed for cylindrical cores of 100 mm in length and 50 mm in diameter. The used pore fluid system was controlled with two pairs of Quizix SP-6000 syringe pumps for up and downstream to ensure continuous fluid flow of aqueous fluids (maximal fluid pressure 140 MPa, maximal flow rate 7.5 ml/min, minimal flow volume 1.77E-7 ml). During the experiments, the confining pressure, axial load, fluid flow, axial and lateral strain, temperature, resistivity, and ultrasonic P- and S-wave velocities were recorded.

### Exposure experiment - first run

For the first run of exposure experiments three BW3 cores were stored with CO<sub>2</sub>-saturated synthetic brine (141.7 g/l chloride, 5.02 g/l sulphate, 91.92 g/l sodium, 3.32 g/l calcium, 1.27 g/l magnesium) in three pressure vessels made of high strength steel with a gas valve (Parker Hannifin GmbH, inner diameter 10 cm, 2 l fluid capacity). To avoid direct contact between brine and vessel material, samples and fluid were placed in a plastic tumbler. Run conditions were 40°C and 6 MPa for a period of six months. Before and after exposure, fluid flow and pressure loading experiments were carried out with the MTS. These experiments were carried out with brine at a constant axial load (4 MPa) and the confining pressure was increased from 0 to 70 in 10-MPa steps. The pore pressure was increased in steps of 2 MPa to 90% of the confining pressure. Fluid flow data, loading pressure, electrical resistivity, and ultra sonic wave velocity were measured.

### Exposure experiment - second run

For the second run, cylindrical cores and pieces from seven Ketzin samples were stored in high-pressure vessels (Fig. 2) made of steel V4A (EN-Norm material number 1.4571X6CrNiMoTi17-12-2, UNS-number S31635). The cores contain trapped formation fluid and can contain trapped Argon from drilling. The vessels were then partly filled with sterile, autoclaved synthetic Ketzin formation fluid (172.854 g/l NaCl, 0.618 g/l, KCl, 8.011 g/l MgCl<sub>2</sub>.6H<sub>2</sub>O and 4.871 g/l CaCl<sub>2</sub>.2H<sub>2</sub>O), pressurized with pure CO<sub>2</sub> to 5.5 MPa, and stored in a heating cabinet at 40 °C. Pore throats and pore size distributions were determined before and after 15 months of CO<sub>2</sub> exposure by mercury injection and Nuclear Magnetic Resonance (NMR), respectively (see below).

### Flow experiment with brine and CO<sub>2</sub>

The flow experiment with brine and CO<sub>2</sub> using the MTS for the outcrop sample S13 of the Stuttgart formation (Table 1) was divided into four phases. The core was originally dry and CO<sub>2</sub> was injected to remove any air. Thus the petrophysical characteristics at CO<sub>2</sub> saturated conditions could be determined. In the first phase brine was injected into the dry CO<sub>2</sub>-saturated sample. Phase II represents a pressure loading experiment on the brine saturated core. In phase III the pressure was released, and CO<sub>2</sub> was re-injected into the brine saturated core. Phase IV represents the pressure loading experiment after the CO<sub>2</sub> flow phase. The entire experiment was carried out at a constant axial load of 4 MPa. During the pressure loading experiments in phase II and IV the confining pressure was increased from 0 to 50 in 10-MPa steps. The pore pressure was increased in steps of 2 MPa to 90% of the confining pressure. Fluid flow data, loading pressure, electrical resistivity, and ultra sonic wave velocity were measured.

## 2.3 Analytical methods

### Mercury injection

Pore throats distributions were derived by measuring mercury injection curves. A Porosimeter 2000 WS with Macro Pore Unit (CE Instruments) was used to analyse vacuum-dried samples of nearly 10 g. The maximum capillary pressure was limited to 200 MPa excluding pores

smaller than 4 nm. The injection curves were used to determine cumulative pore volume, pore throats distributions, bulk density, internal surface area, and mean pore radius. The sample used for mercury injection could not be used for any other measurement because the mercury could not be safely removed.

### Nuclear Magnetic Resonance (NMR)

The nuclear magnetic resonance relaxation time distributions of the transverse (spin-spin)  $T_2$  relaxation was measured on a Maran Ultra Resonance Instrument with 7 MHz for cores up to Ø 40 mm. Simple Carr-Purcell-Meiboom-Gill (CPMG) attenuations of 100% water-saturated core samples with the shortest echo spacing TAU 0.1 ms to minimize the diffusion contrast were recorded. Each CPMG relaxation curve was phase-adjusted and odd-numbered echoes were removed before the Inverse Laplace Transformation (Sørland, 2007). The  $T_2$  relaxation spectra were generated using the WinDXP (Oxford Instruments, UK) software. The permeability was estimated with the Timur-Coates equation (Timur, 1969), which relates the porosity and the free fluid volume ( $T_2 > 33$  ms) to the bound fluid volume ( $T_2 < 33$  ms), where 33 ms is the standard cut off time for sandstone. For spherical pores the relaxation time of a water-wetted pore is proportional to the pore size via surface relaxivity and reflects a distribution of volume to surface of the pores. An average surface relaxivity of 50  $\mu\text{m/s}$  for sandstone was used (Sliikerman, 1998). The pore size distribution determined by NMR generally yields smaller values than the mercury injection derived throat size distribution (see Fleury, 2007; Marschall, 1995).

## 3 Results and Discussion

### 3.1 Petrophysical baseline characterisation

The petrophysical parameters for the outcrop samples of the Stuttgart Formation in Germany and the core samples from Ketzin show overall good consistency (Table 1). The densities determined by helium and mercury injection are comparable and range from 2.5 to 2.8  $\text{g/cm}^3$  for the Ketzin and for the outcrop samples. Likewise, the porosities determined by brine, mercury injection and NMR are comparable and range from 19 to 29 % (mercury injection) 22 to 33.5% (NMR) for the Ketzin samples (the measured 40.1 % for sample B3-3 probably represents an analytical artefact, sample was disintegrated). The Ketzin samples have a relatively large proportion of small pores, as can be seen in the pore size distribution before exposure in Figure 5. The analysed cores sections were taken from the first sandstone horizon of well Ktzi 202 (Fig. 3) and values agree well with the petrophysical and logging data from the other Ketzin wells Ktzi 200 and 201, which show porosities of 5 to > 35 % and permeabilities of 0.02 to > 5000 mD (Norden, 2008).

### 3.2 Exposure experiment first run

To investigate the effects of changed pore space geometry and structure due to  $\text{CO}_2$  injection on ultra sonic wave velocity, electrical resistivity and mechanical properties, brine flow measurements before and after exposure of sandstone samples BW3 to  $\text{CO}_2$ -saturated synthetic brine at in situ conditions were performed.

Figure 4 shows the change of compression wave velocity  $v_p$ , the shear wave velocity  $v_s$ , and Poisson's ratio with increasing pore pressure and confining pressure before and after the exposure. After a time of 6 months no significant changes in flow behaviour were observed.

The compression wave velocity  $v_p$ , and its pressure dependence remained unchanged before and after exposure with a variation of 2%, whereas the shear wave velocity  $v_s$  displayed a higher dependence on pore pressure after exposure. This is also influencing the Poisson's ratio, which increased from 0.30 before to 0.31 to 0.32 after exposure. The P-wave velocity has a high accuracy of 0.01%, whereas the S-wave velocity has a notable lower accuracy due to a large uncertainty of > 5 % in picking the S-waves.

### 3.3 Exposure experiment - second run

Changes in pore throats and pore size distributions of core material from well Ktzi 202 before and after the exposure experiments as determined by mercury injection and NMR, respectively, are shown in Figure 5. The corresponding calculated cumulative porosities are given in Table 1. After 15 months of CO<sub>2</sub>-brine exposure, the porosity of the Ketzin samples as determined by mercury injection ranges from 21 to 33 % and as determined by NMR ranges from 22 to 41 % (Table 1). The porosity increases for samples B2-3, B3-1 and B3-3. However, sample B3-3 is very inhomogeneous as is the case for sample B4-2. Sample B2-2 from the upper most part of the sandstone is more cemented whereas B4-2 from the lower most part is only poorly consolidated. The results from mercury injection and NMR are comparable with smaller porosities determined by mercury injection, except for B3-3. The NMR data generally show a bimodal pore size distribution but indicate a shift in pore radius distribution towards larger pores during the experiments except for B4-2 (Fig. 5). The mercury injection indicates a shift of the larger pores towards smaller pore sizes. This may reflect salt precipitation on surfaces and plugging of pore throats. The core pieces had to be dried for mercury injection without any cleaning with water because they disintegrate then. Therefore, salt precipitation may have occurred during drying.

For all samples, the amount of bound water as determined by NMR relaxation times below 33 ms was estimated to about 75 %. This relatively large value reduced the available volume for the mobile fluid phase. Permeabilities as determined by NMR notably increased after the experiments (except for B4-2). Contrary, NMR data of sample B4-2 indicate a notable shift of the pore size distribution towards smaller pores (Fig. 5d). This may be an effect of the higher magnetic susceptibility and of internal magnetic field gradients reducing the relaxation time (Foley et al., 1996). The X-ray diffraction data from Ketzin sandstones indicate nearly 1% hematite (Norden, 2009), and thin sections indicate partly a ferritic matrix (Kummerow, personal communication). A notably increase in concentration of dissolved Fe (from 30 to 1100 g/l) in sampled brine after injecting supercritical CO<sub>2</sub> into the Frio Formation, Texas USA, was observed by Kharaka et al. (2006). They concluded that the increase in Fe and Mn was caused by dissolution of Fe oxyhydroxides. Carbon dioxide and an acidic pH could be responsible for the dissolution of Fe oxyhydroxides (Wigand et al., 2008).

The measurements show a trend to higher porosities and permeabilities after exposure, but the natural variability for this layered sandstone with layers of mm to cm may be higher than the time depending variations. In batch simulations over 10,000 years for the Utsira reservoir sandstone, Hellevang (2006) found only a slight effect of CO<sub>2</sub> injection on porosity, because porosity increase via the dissolution of primary minerals is accompanied by porosity decrease via the precipitation of secondary silicates and carbonates. Generally Hellevang (2006) found a porosity decrease due to precipitation of CO<sub>2</sub> bearing solids. For CO<sub>2</sub> injection into siliciclastic reservoirs, Xu et al. (2009) simulated a porosity increase close to the well due to

net mineral dissolution but a porosity decrease at greater distance due to mineral trapping. These geochemical simulations predict changes in porosity but cannot directly predict change in permeability, except by applying porosity-permeability relations of the Kozeny-Carman type. The here applied Timur-Coates equation (for the NMR measurements) as well as other comparable relations use the bound water fraction derived from pore size distribution. The change of pore size distribution derived from mercury injection and NMR measurements is therefore a good indicator for permeability variations in cases no direct permeability measurements exist.

### 3.4 Flow experiment with brine and CO<sub>2</sub>

Figure 6 displays the complete flow experiment with brine and CO<sub>2</sub> using the MTS for the outcrop sample S13 of the Stuttgart formation (Table 1). Over the complete experimental time a decrease of resistivity and permeability, and very small changes in ultrasonic wave velocity were observed. Throughout the experiment, the sample was compacted. Because the axial load was held constant, the decrease in sample length (0.24 mm/100 mm) reflects a decrease in the static elastic modulus of the sample. The brine permeability decreases from 2 mD at the beginning to 0.4 mD at the end of the flooding experiment over a period of 10 days. This decrease is probably due to compaction, as volumetric strain measurements indicate a loss of nearly 6% of pore volume. However, this compaction does not reflect CO<sub>2</sub>-brine-rock interaction but rather brine flooding of a core that has been desiccated over a rather long time period. The calculation of ultra sonic wave velocities accounts for this compaction.

#### Phase I - brine injection into CO<sub>2</sub>-saturated core

Phase I of brine injection into the dry CO<sub>2</sub>-saturated sample is shown in Figures 6 and 7. For the dry CO<sub>2</sub>-saturated sample no reasonable ohmic resistance was measurable. Probably, the contact resistance was too high and also the phase difference between current injection (alternating current of 1 kHz) and measured voltage was high. With start of brine injection, the resistivity decreases from 13 to 7 Ωm. The electrical phase changed from 45° to 25°, which is a usual value for fluid filled pores at this measurement configuration. The observed phase shift indicates a higher capacitive fraction at dry, CO<sub>2</sub>-filled conditions without any electrolytic conductivity.

The ultrasonic compression wave velocity  $v_p$  of the dry sample saturated with CO<sub>2</sub> is 2.57 km/s and increased at brine saturation by about 14 % to 3.00 km/s at the same pressure conditions. The ultrasonic shear wave velocity  $v_s$  varied only a little.

#### Phase III - CO<sub>2</sub> injection into brine saturated core

After the pressure loading experiment of Phase II (see below) the pressure was again reduced, and the changes caused by CO<sub>2</sub> injection in a brine saturated sample were investigated (Figures 6 and 7; Phase III 7200-8600 min). Because the used Quizix pumps are not suitable for gas, a CO<sub>2</sub> gas bottle with a constant CO<sub>2</sub> pressure at 0.2 MPa was used. Therefore no data on flow rate and volume are available. A confining pressure of 10 MPa and an axial load of 4 MPa were applied. This experiment shows that during the injection of CO<sub>2</sub> into the brine saturated sample (Figure 7) the velocity of the compression wave  $v_p$  decreases from ~ 3.00 km/s to ~ 2.92 km/s (3%), while the shear wave velocity  $v_s$  increases very slightly from ~ 1.630 km/s to ~ 1.636 km/s. Xue and Ohsumi (2004) reported, that the P-wave velocity



decreases by about 4.3 to 6.5% of the initial velocity after injection of gaseous CO<sub>2</sub> into a water saturated sandstone. The impact of the CO<sub>2</sub> on velocity is smaller in our experiment, which is probably due to a partial displacement of brine and high residual water saturation. The velocity of the dry CO<sub>2</sub> saturated core at the beginning was 2.57 km/s. The effect of CO<sub>2</sub> on seismic velocities is caused through the changes of the bulk modulus of the pore space as gas saturation changes and dissolving gas in the fluid and changing bulk density of the rock, and is described by the so-called Gassmann equation (Gassmann, 1951; Hoversten, 2003). Electrical measurements indicate two phase flow conditions. Overall, during the CO<sub>2</sub> flow the phase change is 80° and the calculated resistivity is 0.3 Ωm, which are unexpected values. However, some scattered values have normal phases with resistivity between 17 and 19 Ωm compared to 5 Ωm at brine flow conditions. This suggests a CO<sub>2</sub> saturation of 50% according to Archie's law.

#### Phase II and IV- comparison of pressure loading at brine saturation

For the repeat of the pressure loading experiment, brine was again injected and then the same pressure loading started as in Phase II (Figure 6 from 8600 min).

Figure 8 compares of the measured P- and S-wave velocities before (Phase II) and after (Phase IV) the CO<sub>2</sub> exposure as function of pore pressure. The velocities are strong functions of pore and confining pressure, because increasing pore pressure decreases the effective loading, and thus increases porosity and also change, e.g., grain contacts (Christensen, 1985, David, 1993). The differences in ultrasonic wave velocities before and after exposure are, however, only minimal.

#### **4**      *Summary*

The brine flow experiments before and after CO<sub>2</sub> exposure, which were conducted over several months under reservoir conditions with brine and CO<sub>2</sub> on sandstones of the Stuttgart formation, showed no significant changes of velocity and resistivity at brine flow conditions.

The batch experiments on sandstone samples from Ketzin, which were conducted over 15 months under reservoir conditions with brine and CO<sub>2</sub>, showed a slightly increased porosity. The pore size distribution derived from NMR measurements shows a shifting to larger pore size. The measured porosity increase is in the same order as the naturally variability of this layered sandstone. Further analyses after even longer run durations and the comparison with geochemical and petrological as well as fluid analysis are pending.

The flow experiment with brine and CO<sub>2</sub> shows a dependence of pore fillings for resistivity and P-wave velocity and no significant change of shear wave velocity. The velocity of P-wave increase by about 14% of initial velocity at brine flooding in a CO<sub>2</sub> saturated core, and decrease by about 3% of initial velocity from CO<sub>2</sub> flooding in a brine saturated core. This small change indicates high residual water saturation, and a residual water saturation of 50% results from electrical measurements. The sample was compacted over the experimental time of 2 weeks under constant axial loading. This compaction and the reduction of flow rate and brine permeability indicate alteration in structure and porosity and overlay the other effects. Pressure loading experiments before and after CO<sub>2</sub>-flow phase show no significant change in the dependence of velocities from pore pressure. The experimental time of CO<sub>2</sub> flow phase was too short for alterations induced by CO<sub>2</sub>-brine rock interaction.

The dissolution/precipitation of minerals and possible textural modifications (shale

mobilisation, cement, porous network) induce important changes in both the physical (e.g. evolution of the porosity and permeability) and mechanical behaviours of the reservoir rocks. These modifications are not yet understood in detail.

## **5 Outlook**

Studies of the fluid composition and mineralogical changes in the core material before and after the exposure experiment are currently underway. The exposure experiment is going on, and there will be new samplings every four to six months. The rates of fluid-rock reaction can be relatively slow, and so it may take several months (or longer) for significant fluid-rock reactions to occur. Experiments on samples of the Utsira Sand conducted over timescales of up to two years showed relatively little reaction - during the first two months equilibration of carbonate mineral reactions predominated, while reactions between silicate minerals were still ongoing (Rochelle et al., 2002).

Additional flow experiments for determining of reservoir parameters (permeability) and geomechanical testing for mechanical stability are also planned. These planned flow measurements of Ketzin samples before and after the exposure experiments at the MTS are exceedingly difficult, because the collected sandstone samples are very unstable, and some cores underwent shear fracture during axial loading at 0.2 MPa. A report of the flow experiments under reservoir conditions with Ketzin cores with another size in another testing system (without strain measurement and axial loading) is in preparation (Kummerow, personal communication).

## **Acknowledgements**

The CO<sub>2</sub>SINK project receives its funding from the European Commission FP6, the Federal Ministry of Economics and Technology BMWi, and the Federal Ministry of Education and Research BMBF. We thank the Institute of Petroleum Engineering of TU Clausthal for providing the NMR-Tomograph and Juliane Kummerow for providing data for the new Ketzin samples. Liane Liebeskind assisted us with the experiments using the triaxial cell.

## **References**

- Brosse, E., Bildstein, O., Swennen, R., 2005. Gas-Water-Rock interactions induced by reservoir exploitation, CO<sub>2</sub> Sequestration, and other geological storage. *Oil & Gas Science and Technology – Rev. IFP*, Vol. 60, No. 1, 9-18.
- Christensen, N. I., Wang, H. F., 1985. The influence of pore pressure and confining pressure on dynamic elastic properties of Berea sandstone. *Geophysics*, 50 207-213.
- David, C., Darot, M., Jeannette, D., 1993. Pore structures and transport properties of sandstone. *Transport in Porous Media* 11, 161-177.
- Fleury, M., 2007. NMR surface relaxivity determination using NMR apparent diffusion curves and BET measurements. *Society of Core Analysts*, SCA2007-35.
- Foley, I., Farooqui, S. A., Kleinberg, R. L., 1996. Effect of paramagnetic ions on NMR relaxation of fluids at solid surfaces. *Journal of Magnetic Resonance* (123), 95-104.

- Förster, A., Norden, B., Zinck-Jørgensen, K., Frykman, P., Kulenkampff, J., Spangenberg, E., Erzinger, J., Zimmer, M., Kopp, J., Borm, G., Juhlin, C., Cosma, C. and Hurter, S., 2006. Baseline characterization of the CO<sub>2</sub>SINK geological storage site at Ketzin, Germany. *Environmental Geosciences*, Vol. 13, No. 3.
- Förster, A., Giese, R., Juhlin, C., Norden, B., Springer, N. and CO<sub>2</sub>SINK Group, 2008. The geology of the CO<sub>2</sub>SINK site: from regional scale to laboratory scale. *Energy Procedia*
- Förster, A., Vu-Hoang, D., Marcelis, F., Springer, N., Le Nir, I., 2008. Lithological and petrophysical core-log interpretation in the CO<sub>2</sub>SINK, the European CO<sub>2</sub> onshore research storage and verification project. SPE 115247 SPE Asia Pacific Oil and Gas Conference and Exhibition (Perth, Australia 2008).
- Gassmann, F., 1951, Über die Elastizität poröser Medien: *Vierteljahresschrift der Naturforschenden Ges.*, Zürich, 96, 1–23.
- Hellevang, H., 2006. Interactions between CO<sub>2</sub>, saline water and minerals during geological storage of CO<sub>2</sub>. Thesis (PhD) University of Bergen, Norway.
- Hoversten, G. M., Gritto, R., Washbourne, J., Daley, T., M., 2003. Pressure and fluid saturation prediction in a multicomponent reservoir, using combined seismic and electromagnetic imaging: *Geophysics*, 68, 1580-1591.
- Hovorka, S.D., 2004. Frio Brine Pilot experiment – Update and preliminary results. Presented at the Geological Society of America Annual Meeting: Denver, Colorado, Nov. 7-10.
- Kharaka, Y.K., Cole, D.R., Hovorka, S.D., Gunter, W.D., Knauss, K.G., Freifeld, B.M., 2006. Gas–water–rock interactions in Frio formation following CO<sub>2</sub> injection: implications for the storage of greenhouse gases in sedimentary basins. *Geology* 34.
- Kleinberg, R. L., 1996. Utility of NMR T2 distributions, connection with capillary pressure, clay effect, and determination of the surface relaxivity parameter  $\rho$ . *Journal of Magnetic Resonance* 14, 761-767.
- Marschall, D., Gardner, J.S., Mardon, D. and Coates, G.R., 1995. Method for correlating NMR relaxometry and mercury injection data. *Trans. International Symposium of the SCA*, San Francisco, California. Sept. 12-15, 1995.
- Norden, B., Förster, A., Vu-Hoang, D., Marcelis, F., Springer, N., Le Nir, I., 2008. Lithological and Petrophysical Core-Log Interpretation in CO<sub>2</sub>SINK, the European CO<sub>2</sub> Onshore Research Storage and Verification Project. SPE Asia Pacific Oil and Gas Conference and Exhibition, 2008, Perth, Australia.
- Pearce, J.M., Czernichowski-Lauriol, I., Rochelle, C.A., Springer, N., Brosse, E., Sanjuan, B., Bateman, K., and Lanini, S., 2000. How will reservoir and caprock react with injected CO<sub>2</sub> at Sleipner? Preliminary evidence from experimental investigations. 5th International Conference on Greenhouse Gas Control Technologies, Cairns (Australia), August 2000.
- Rochelle, C.A., Bateman, K., Pearce, J.M., 2002. Geochemical interactions between supercritical CO<sub>2</sub> and the Utsira formation: An experimental study. *British Geological Survey Commissioned Report*, CR/02/060.
- Rochelle, C.A., Czernichowski-Lauriol, I., Milodowski, A.E., 2004. The impact of chemical reactions on CO<sub>2</sub> storage in geological formations: a brief review. In: Baines, S.J., Worden, R.H. (Eds.), *Geological Storage of Carbon*.

Schütt, H., Wiegand, M., Spangenberg, E., 2004. Geophysical and geochemical effects of supercritical CO<sub>2</sub> on sandstones, in: D. C. Thomas, and S. Benson (eds.), Carbon Dioxide Capture for Storage in Deep Geologic Formations – Results from the CO<sub>2</sub> Capture Project, v. 2, Amsterdam, Elsevier, pp. 767–786.

Slijkerman, W.F.J. and Hofman, J.P., 1998. Determination of surface relaxivity from NMR diffusion measurements. *Journal of Magnetic Resonance* 16, 541-544.

Sørland, G.H., Djurhuus, K., Widerøe, H. C., Lien, J.R. and Skauge, A., 2007. Absolute pore size distribution from NMR. *Diffusions Fundamentals* 5.

Timur, A., 1969. Productible porosity and permeability of sandstones investigated through NMR principles. *Log Analyst*, 10(1), 3-11.

Wandrey, M., Morozova, D., Zettlitzer, M., Würdemann, H., and the CO<sub>2</sub>SINK Group, 2010. Assessing drilling mud and technical fluid contamination in reservoir rock and brine samples from the Ketzin storage site using fluorescent dye tracers. *International Journal of Greenhouse Gas Control*, accepted.

Wigand, M., Carey, J., Schütt, H., Spangenberg, E. and Erzinger, J., 2008. Geochemical effects of CO<sub>2</sub> sequestration in sandstones under simulated in situ conditions of deep saline aquifers. *Applied Geochemistry* 23.

Worden, R.H., and Smith, L.K., 2004. Geological sequestration of CO<sub>2</sub> in the subsurface: lessons from CO<sub>2</sub> injection enhanced oil recovery projects in oilfields. In: Baines, S.J., and Worden, R.H. (eds), *Geological Storage of Carbon Dioxide*. Geological Society, London, Special Publications, 233, 211-224.

Würdemann, H., Schilling, F., Möller, F., Kühn, M., 2009. Status Report on the First European on-shore CO<sub>2</sub> Storage Site at Ketzin (Germany). *Geophysical Research Abstracts*, Vol. 11, EGU2009-13724.

Xiao, Y., Xu, T., Pruess, K., 2009. The effects of gas-fluid-rock interactions on CO<sub>2</sub> injection and storage: insights from reactive transport modelling. *Energy Procedia* 1, GHGT 9.

Xue, Z., Ohsumi, T., 2004. Seismic wave monitoring of CO<sub>2</sub> migration in water-saturated porous sandstone. *Explorations Geophysics* 35, 25-32.

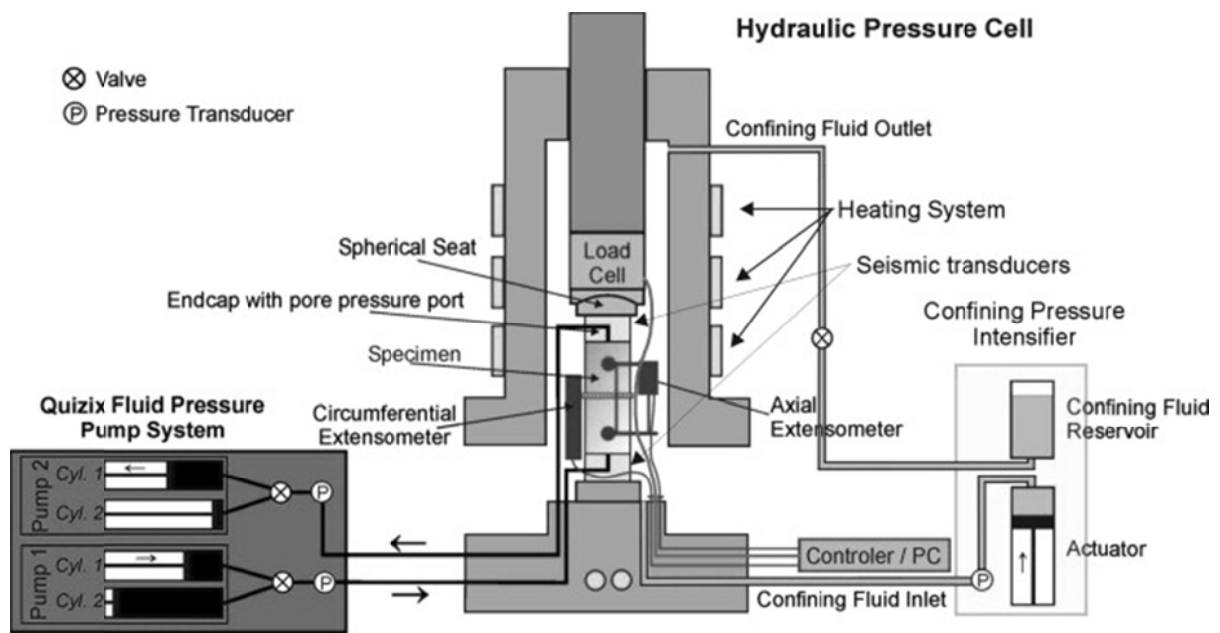


Fig. 1 Sketch of triaxial cell with the pump and heating system (Schütt et al., 2004).



Fig. 2 Corrosion-resistant, high-pressure vessels with a gas valve for cores, with an inner diameter of 60 mm and a length of 140 mm, designed for pressures up to 10 MPa.

Table 1 Petrophysical properties of Stuttgart Formation samples.

Stuttgart formation	Bulk density [g/cm <sup>3</sup> ]		Porosity [%]			Spez. Surf. [m <sup>2</sup> /g]	Mean pore radius [μm]	Permeability [mD]		Formation factor	Velocity [m/s] (100% brine)	
	He	Hg	brine	NMR	Hg	Hg	Hg	brine	NMR Coates		v <sub>p</sub>	v <sub>s</sub>
<b>Outcrops of Stuttgart formation Germany</b>												
<b>S9</b> Herrmannsberg	2.65	2.60		22.7	17.3	1.78	4.86		53			
<b>S14</b> Ansbach	2.72	2.59		29.1	28.2	4.68	6.05		39			
<b>S13</b> Friedrichsberg	2.76	2.59		22.98	17.1	3.71	3.91	2	8	6.37	3000	1540
<b>GR</b> Gispersleben red	2.79	2.61		26.0	25.3	3.12	3.91		13		2800	1500
<b>GG</b> Gispersleben grey	2.73	2.52			18.2	4.21	2.27				2800	1500
<b>BW3</b> Baden Württemberg	2.66	2.66			19.1	2.58	5.12	30 100		14.7	2950	1510
<b>Ktzin 202 core samples prior to CO<sub>2</sub> exposure</b>												
<b>B2-2</b> 627.3-628.3 m	2.64	2.8		19.0	22.5	1.87	6.0		40			
<b>B2-3</b> 628.3-629.2 m	2.67 2.62	2.7	28.1 27.6	27.9 29.2	22.7	0.80	8.1		41 40			
<b>B3-1</b> 629.2-630.3m	2.61	2.50	28.5	27.1	24.9	1.24	7.5		12			
<b>B3-3</b> 631.3-632.3 m	2.58	2.6	28.3	25.9 28.5	28.0 40.6	1.15 1.61	10.1 10		18 96			
<b>B4-2</b> 633.1-634.1 m	2.60	2.8	27.8	26.9	33.5	1.04	11.5		62			
<b>Ktzin 202 core samples after 15 months CO<sub>2</sub> exposure</b>												
<b>B2-2</b>		2.9		20.8	22.4	2.4	7		22			
<b>B2-3</b>		2.5		30.5 30.3	25.2	1.7	8.6		158 194			
<b>B3-1</b>		2.9		31.9	34.1	2.9	9		192			
<b>B3-3</b>		2.0		32.9	41.3		15		491			
<b>B4-2</b>		-		27.5	-		6		7			

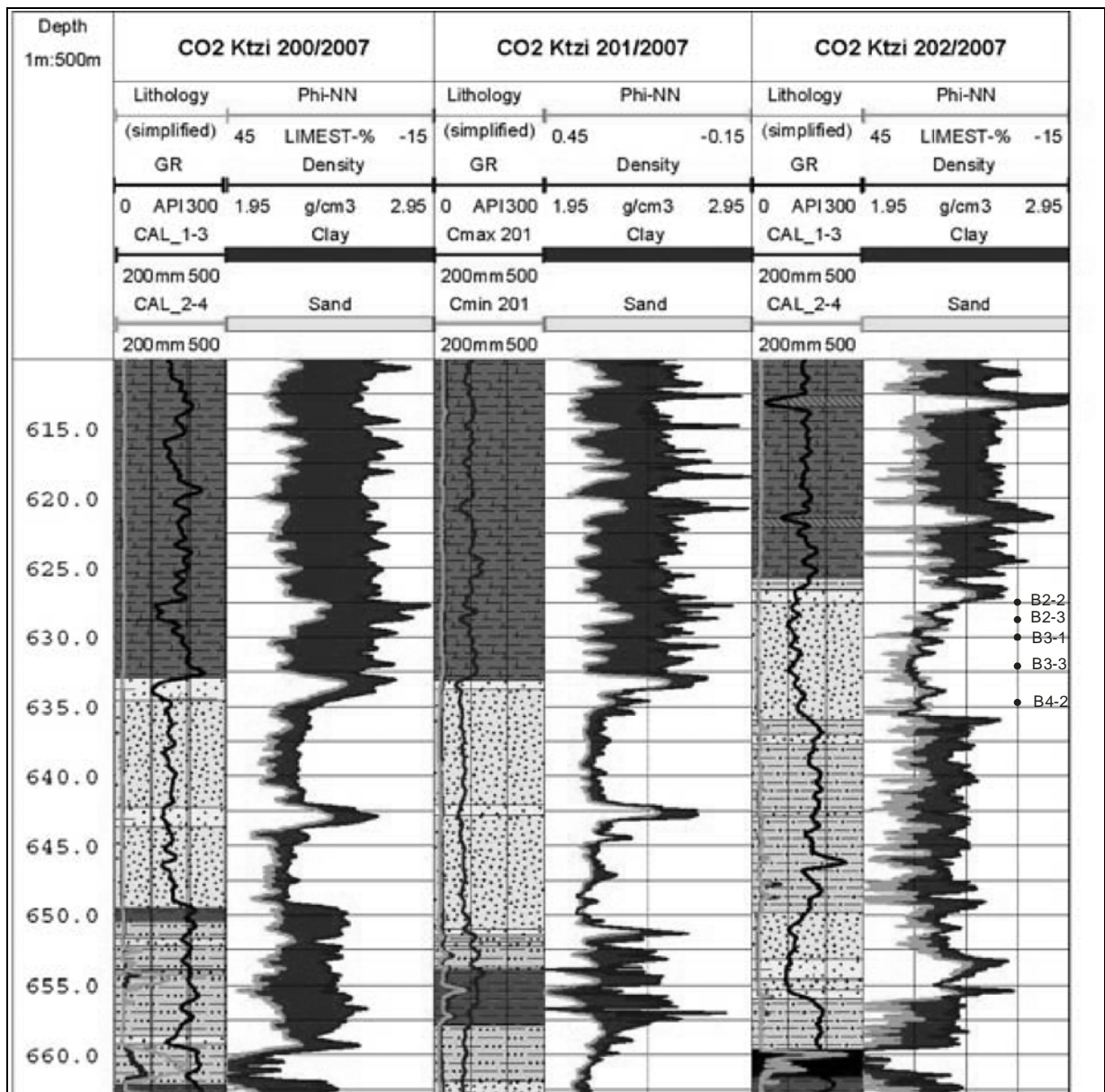


Fig. 3 Simplified litho-logs for Stuttgart Formation section (after Förster et al., 2008).

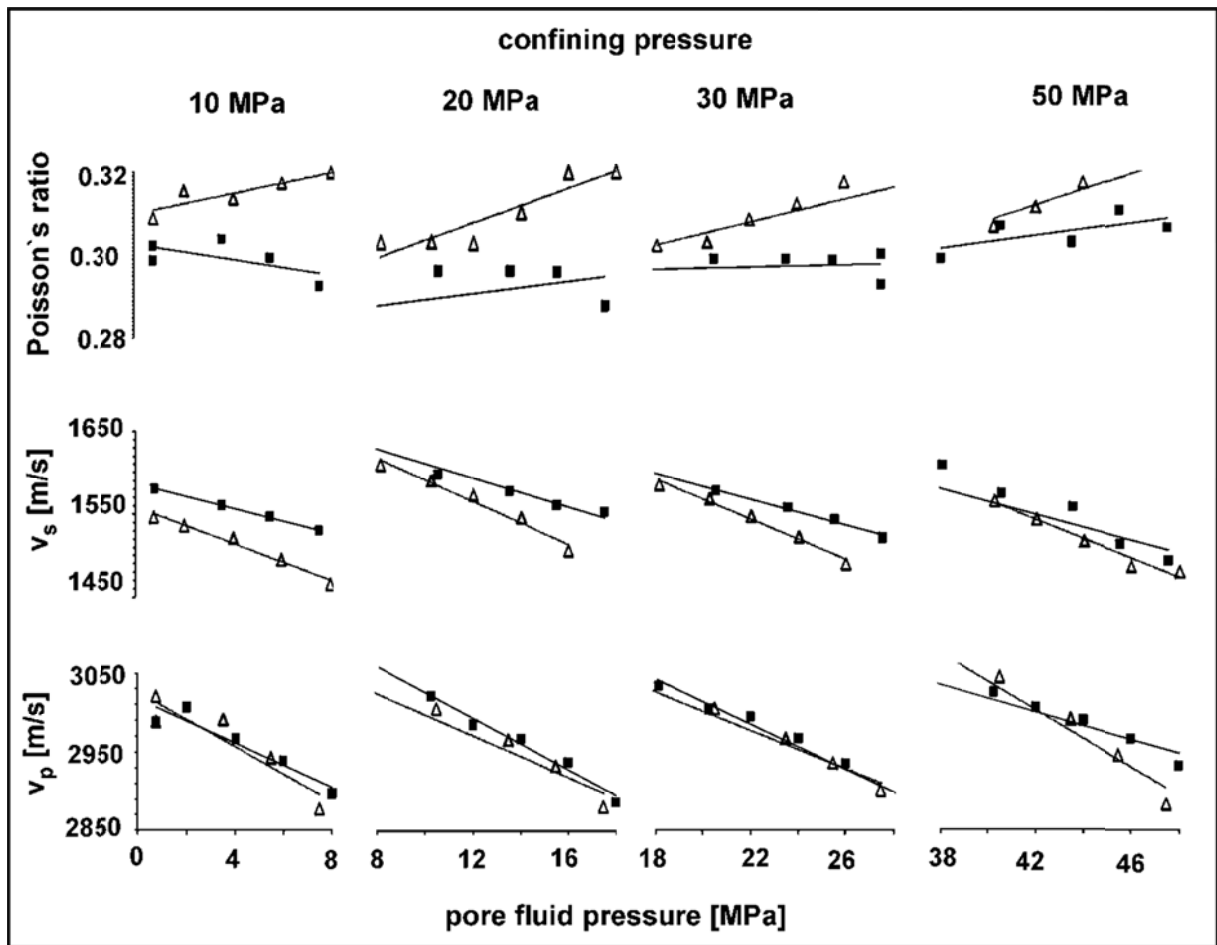
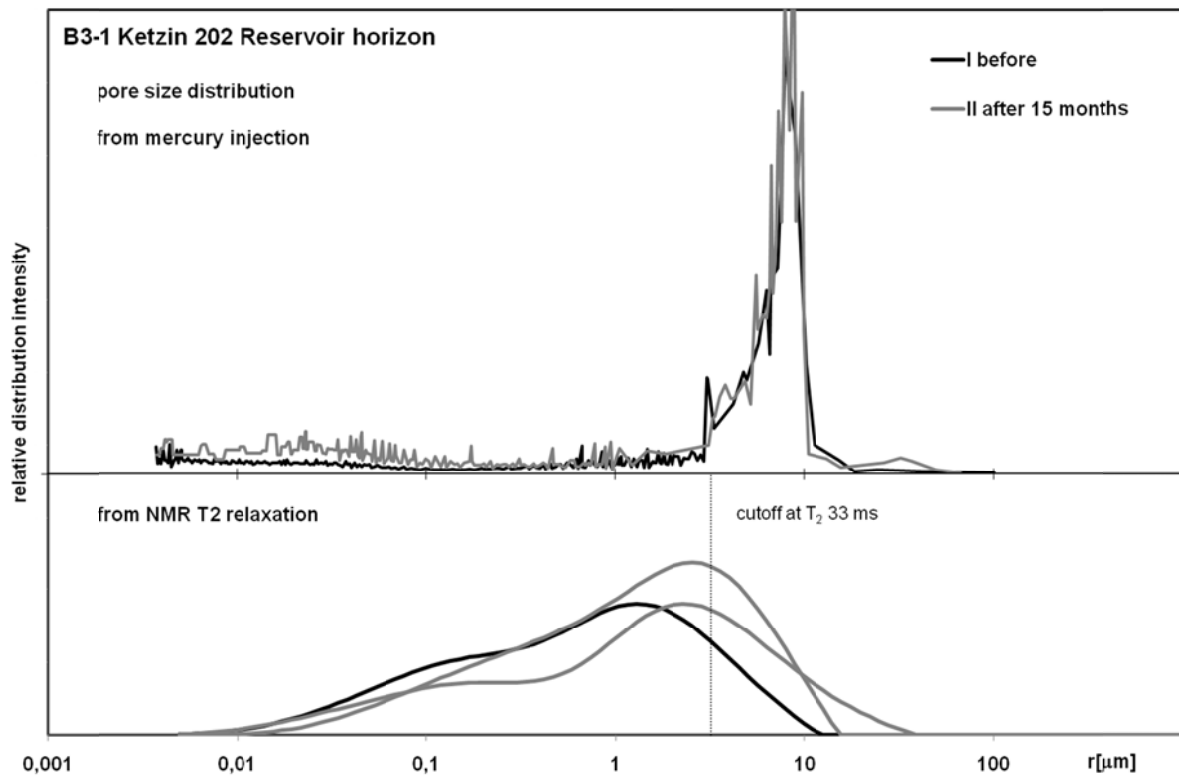
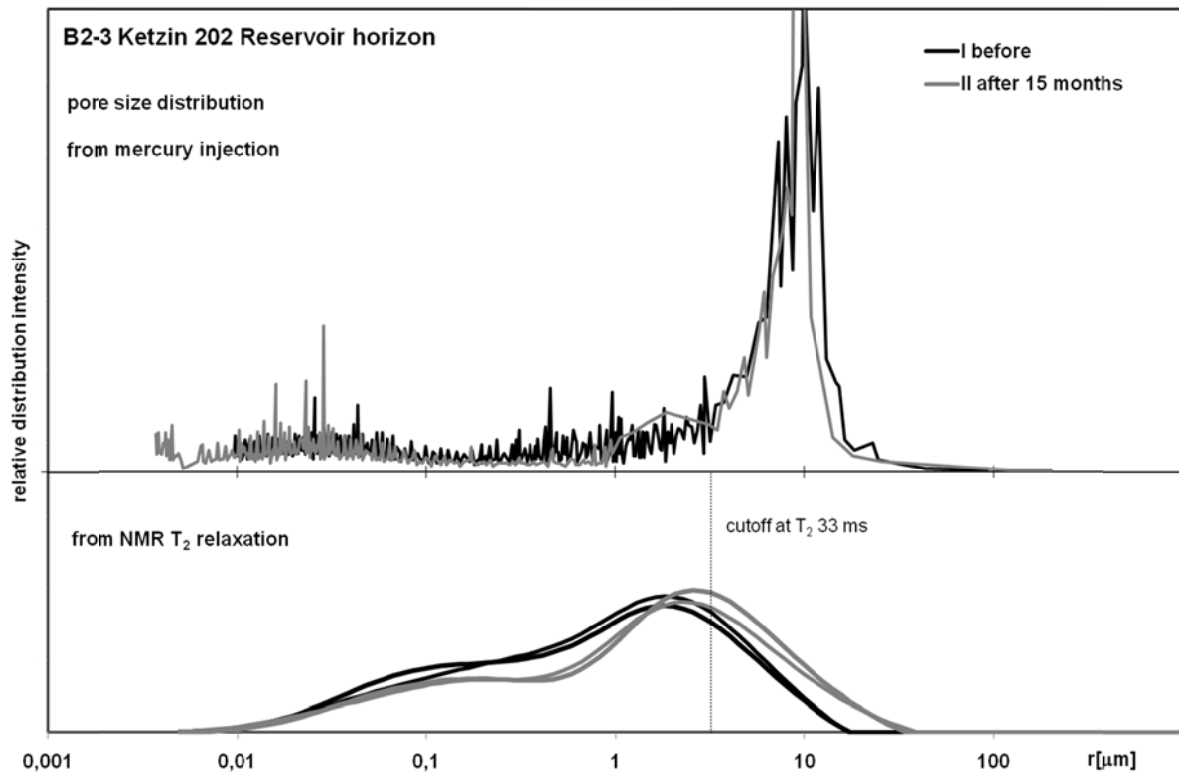


Fig. 4 Velocity ( $v_p$  and  $v_s$ ) as a function of pore and confining pressure (BW3)

Black rectangles: Sampel A before

Empty triangles: Sample B after six months of CO<sub>2</sub> exposure





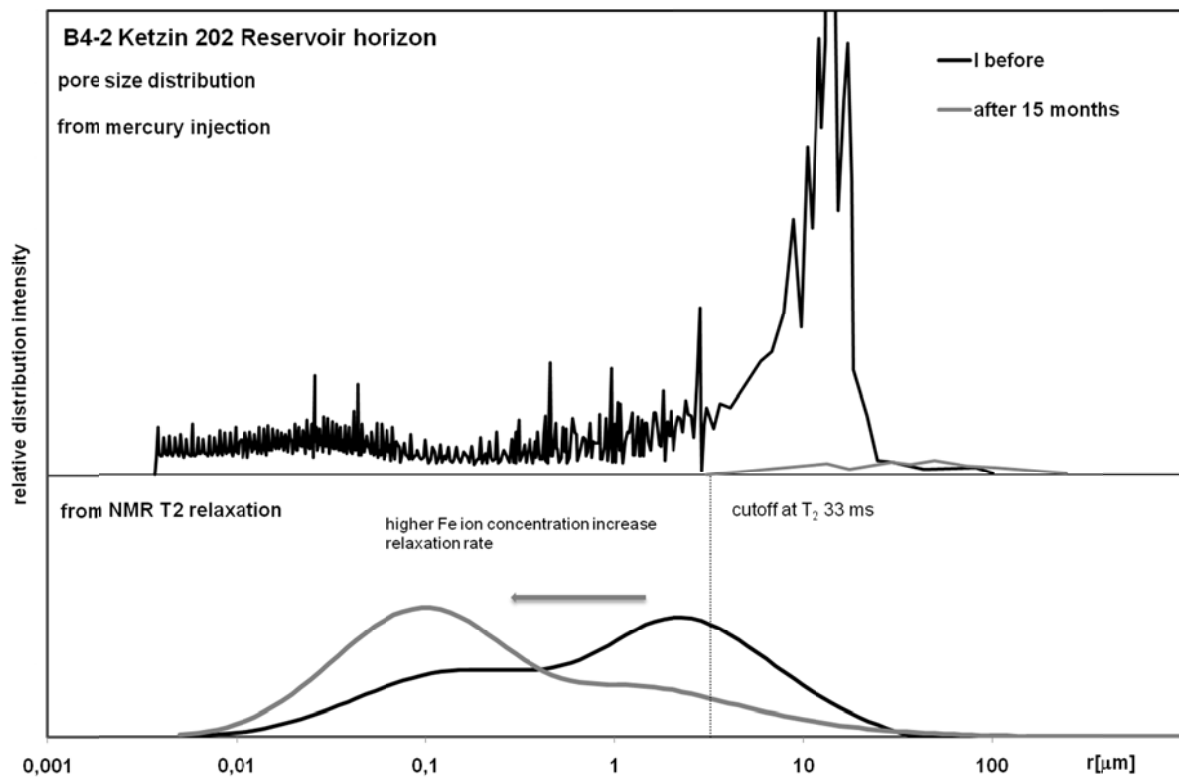
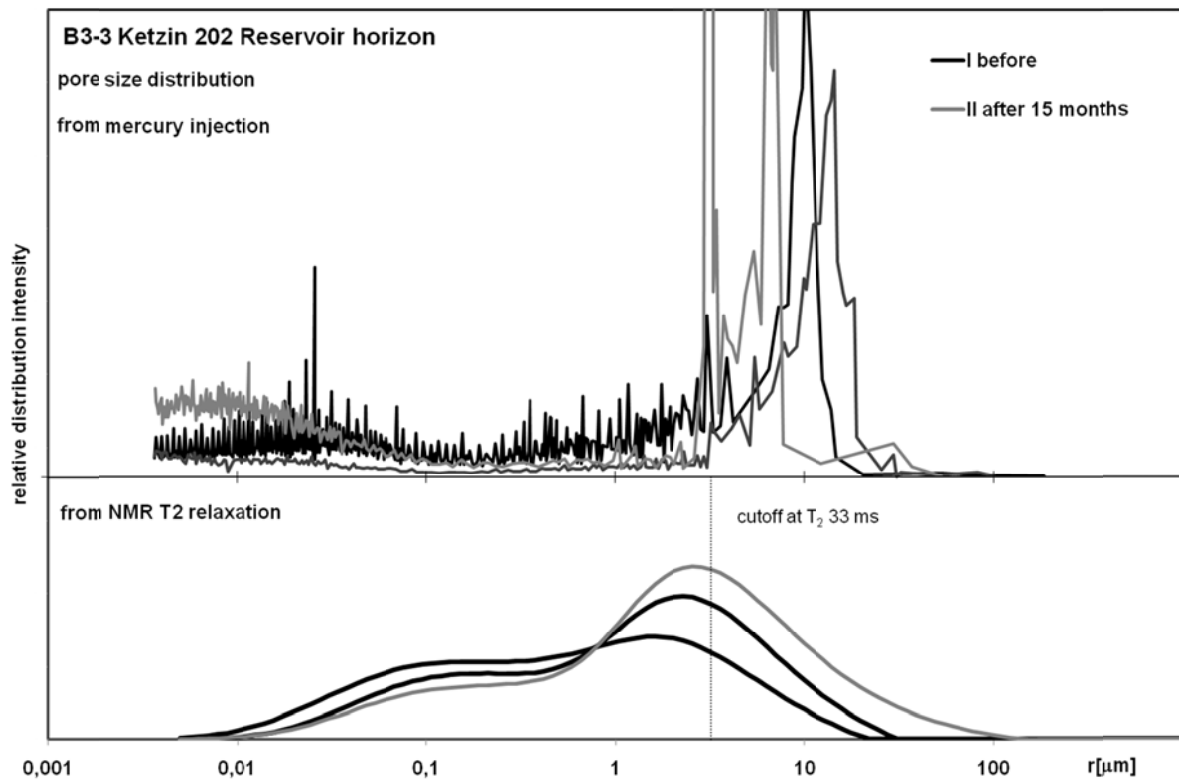


Fig. 5a-d Pore size distributions before and after 15 months CO<sub>2</sub> exposure  
 pore throats distribution derived from mercury injection and  
 pore size distribution derived from NMR T<sub>2</sub> measurements

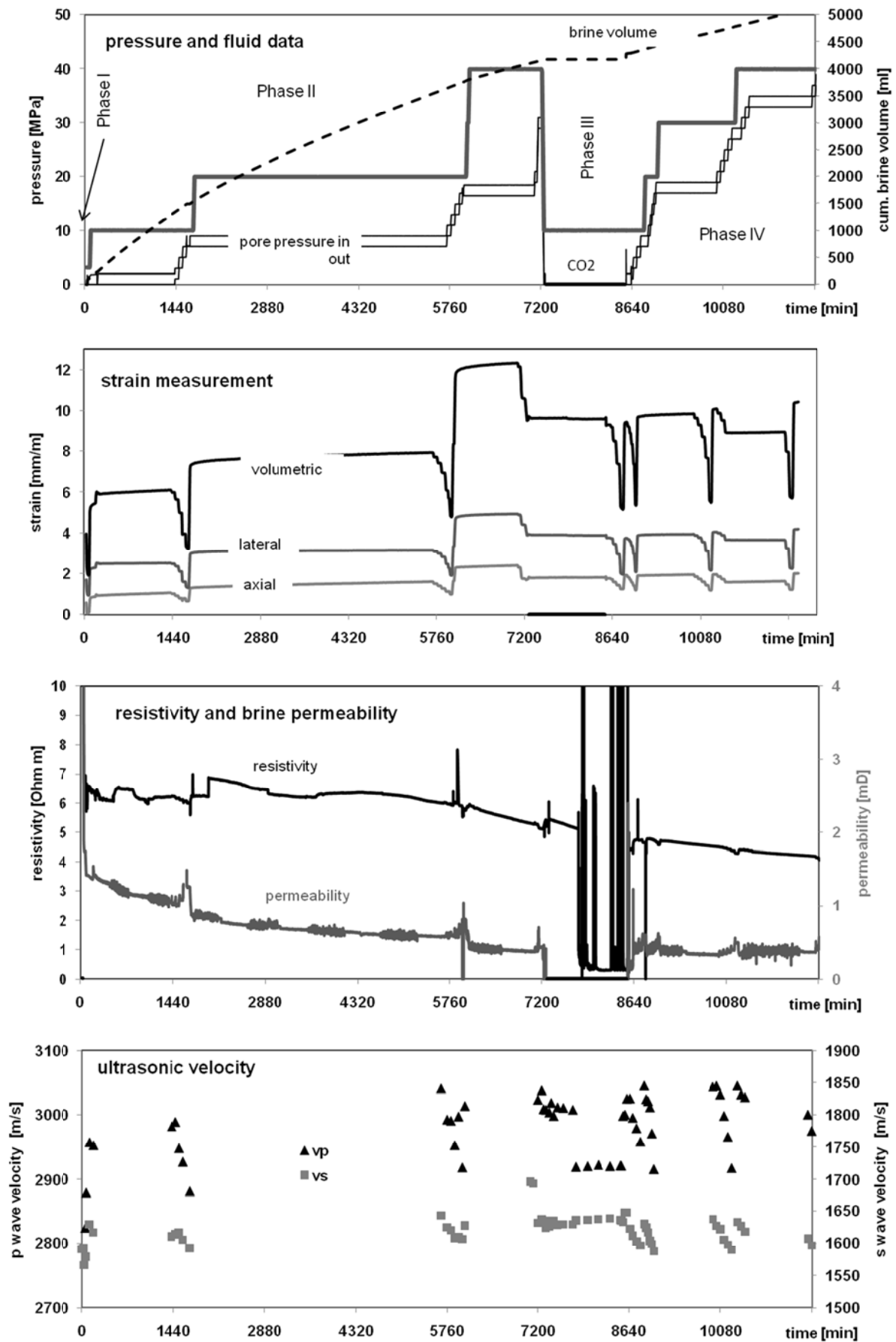


Fig. 6 Flow experiments with brine/CO<sub>2</sub> on sandstone sample S13.

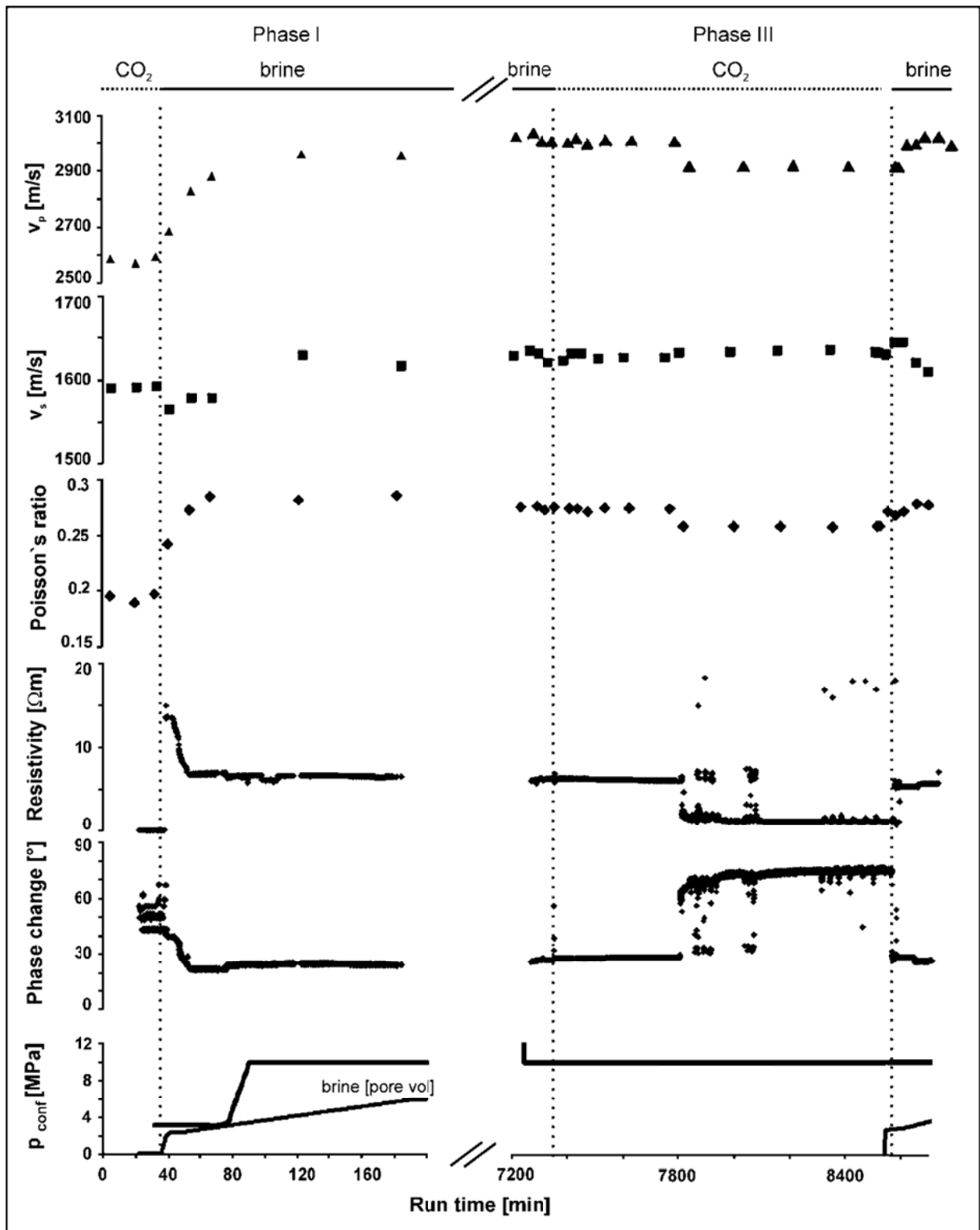


Fig. 7 Changes in ultrasonic velocities/Poisson's ratio and resistivity / el. phase during  
Phase I: brine injection into CO<sub>2</sub>-saturated sample  
Phase III: CO<sub>2</sub> injection into brine-saturated sample

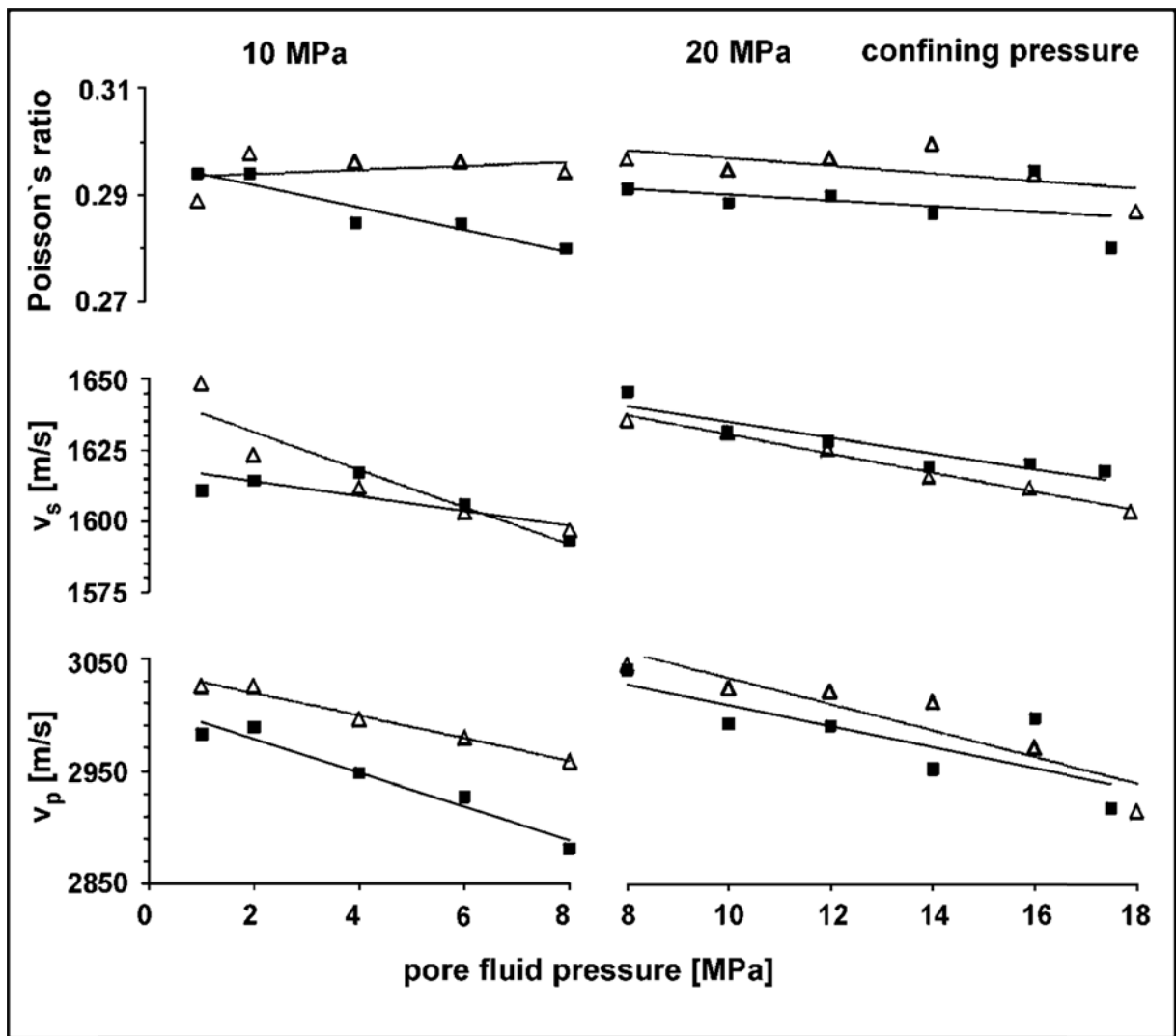


Fig. 8 Velocity ( $v_p$  and  $v_s$ ) / Poisson's ratio as a function of pore and confining pressure during pore pressure increasing at confining pressure steps

Black rectangles: Phase II

Empty triangles: Phase IV after CO<sub>2</sub> exposure